An Artificial Intelligent Hybrid Controller for Solar and Battery Fed Five-Level UPQC for Power Quality Improvement

Guguloth MohanBabu *, G. Suresh Babu **, E. Vidya Sagar *

* Department of Electrical Engineering, Osmania University, Hyderabad, Telangana, India.

** Department of Electrical and Electronics Engineering, Chaitanya Bharathi Institute of Technology, Telangana

(mohanbabuguguloth1985@gmail.com, gsureshbabu_eee@cbit.ac.in , evsuceou@gmail.com)

‡ Corresponding Author: Guguloth MohanBabu, Department of Electrical Engineering, Osmania University, Hyderabad, Telangana, India, Tel: +91-8328180776,

mohanbabuguguloth1985@gmail.com.

Received: 07.07.2023 Accepted:03.08.2023

Abstract: This study examines the diode-clamped five-level unified Power quality conditioner coupled with photovoltaic and battery storage systems to handle the power quality related problems. The traditional SRF and p-q theories require the transformations like abc, dq0, αβ etc to generate reference signal generation. In this paper, eliminates that conventional complex transformations and adopts the artificial neural network-based control scheme with levenberg- marquardt back propagation training method is adopted for the diode clamped 5L-UPQC to generate the necessary reference signals for the voltage source converters. In addition, an adaptive neuro-fuzzy interface system hybrid controller is suggested for DC link error current minimization, which adapts both the properties of fuzzy and ANN. The prime goal of the developed scheme is to maintain constant DLCV during load changes, diminish of total harmonic distortion in the source current and load voltage waveforms, and maximum elimination of source voltage distortions like sag/swell and disturbances. The suggested method was demonstrated in two cases with various combinations of loads. However, to exhibit the performance of the proposed technique, the comparison is carried out with the ANN, PIC and SMC.

Keywords- Unified Power Quality Conditioner, Total Harmonic Distortion, Power Quality, Shunt Active Power Filter, and Series Active Power Filter

Nomenclature:

Five-level-UPQC	5L-UPQC
PV	Photovoltaic
PQ	Power Quality
SRF	Synchronous reference frame theory
p-q	Instantaneous reactive power theory
ANN	Artificial neural network
LMBP	Levenberg- marquardt back propagation
DLCV	Direct current link capacitor voltage
THD	Total harmonic distortion
PF	Power factor
GA	Genetic algorithm
PSO	Particle swarm optimization
PIC	Proportional integral controller
SHAPF	Shunt Active Power Filter
GWO	Grey wolf optimization
BC	Boost converter
PWM	Pulse width modulation
BSS	Battery system storage
SMC	Sliding mode control

FLC	Fuzzy logic controller
VSC	Voltage source converter
BBC	Buck-boost converter
UPQC	Unified Power quality conditioner
MSE	Mean square error
BBO	Biogeography based optimization
SEAF	Series Active Power Filter
ACO	Ant colony algorithm
FOPID	Fractional order proportional integral derivate
MSF	Membership function
ANFIS	Artificial neuro-fuzzy interface system
FF-ANN	Firefly based ANN
PPFFA	Predator-prey firefly algorithm
SPG	Solar power generation
V_{LL}	Line to Line rms voltage
CE	Change in error
OL	Output Layer of ANN
IL	Input layer of ANN
HL	Hidden layer of ANN
E	Error
m	Modulation index
$V_{cr,pp}$	Peak-to-peak voltage ripple
$i_{BS,er}^{*}$	Battery reference error current
Δi_{lmax}	Peak ripple current
V_m	Peak voltage of the system
a_f	Overloading factor
i_{l_abc}	Load current for abc phases
f_{sh} f_{se}	Switching frequency
L_{se}	SEAF Inductance
V_{S_abc}	Source voltage for abc phases
R_S , L_S	Grid Resistance and Inductance
V_{l_abc}	Load voltage for phases a, b, c
C_{dc}	DC link capacitance
V_{se_abc}	Series injected voltage for phases a, b, c
$V^{ref}{}_{se\_abc}$	Reference Series injected voltage for phases a, b, c
i_{S_abc}	Source current for abc phases
R_{sh}	SHAPF Resistance
V_{dc}	DC link voltage
$V^{ref}{}_{dc}$	Reference DLCV
Δi_{dc}	DC link output error
i_{sh_abc}	SHAPF injected current in abc phases
$i^{ref}{}_{BS}$	Battery reference current
$i^{ref}{}_{sh\_abc}$	Reference SHAPF injected current in abc phases
$i^{ref}{}_{dc}$	Reference DC current
R_{se}	SEAF Resistance
$V_{dc,err}$	DLCV error
$i_{BS,err}$	Battery error current
i_{ph}	photocurrent source
L_{sh}	SHAPF Inductance
i_d	Forward diode carrying current
$R_{s,PV}$ and $R_{sh,PV}$	Series and parallel cell resistances of PV

1. Introduction

In recent years, integrating renewable energy systems like solar and wind into the distribution network has been encouraged to reduce the stress on converters and ratings. The solar-integrated UPQC was developed to address PQ issues efficiently. In addition, a novel fuzzy-based proportional integral controller was designed for the Maximum power tracking technique to extract maximum power and balance DLCV [1]. Besides, a new hybrid enhanced method associated with the ANN technique for the SHAPF was introduced to reduce the imperfections in current waveforms and improve the PQ in the distribution network [2]. Next, the PSO and GWO-based optimal SHAPF was designed with the optimal tuning of FOPIDC for reactive power handling and compensation of harmonic components with an experimental investigation [3]. However, the performance of wind systems connected to UPQC was studied on different loads and faulty conditions by adopting hysteresis and PWM techniques [4]. Further, the power flow analysis of the UPQC was analyzed on a three-phase distribution system with various faculty conditions from the point of impedance matching technique [5].

The various existing algorithms for controlling the operation of SHAPF and harmonics isolation techniques, DLCV regulation, and current control methods are discussed [6]. A new metaheuristic HBO was proposed from the intelligent hunting behavior of honey badgers with a motive for solving optimization problems. Besides, the fuzzy-based hybrid technique was adopted to achieve maximum out of PV. However, to reduce the complexity the ANN was considered for UPQC reference signal generation to sole PQ issues [7]. The intelligent fuzzy-tuned proportional integral controller PIC was designed for the hybrid shunt active and passive filters to minimise the current THD. However, the performance analysis was carried out for varying loads using Clarke's transformation [8]. Meanwhile, by adopting ANN, the Solar PV powered UPQC was presented to reduce grid current THD during voltage fluctuations like sag, and swell. In addition, the proposed method was compared with SRF and reactive power theory methods under varying load conditions [9]. The Modified Shuffled Frog Leaping Algorithm (MSFLA) based optimal allocation of D-STATCOM and DG was suggested for the IEEE 33 node system with an objective of reducing system energy losses and costs [10].

Besides, to regulate DLCV and to handle reactive power feed forward ANN was suggested for PV/wind associated UPQC [11]. The H bridge inverter-based single phase SHAPF with a modified Predictive Current Control method was introduced to reduce THD in grid current waveform [12]. Future, the microgrid-connected multilevel DSTATCOM was developed to eliminate voltage and current distortions effectively [13]. Besides, a comprehensive study was done on various phase synchronisation techniques used to control the working of SHAPF [14]. The novel load equivalent conductance technique was introduced for the UPQC to improve power quality to regulate energy transfer between sources and loads [15].

Intelligent hybrid controllers like fuzzy-PIC and fuzzy proportional integral derivative controllers were proposed for the AC-DC micro-grid system to improve voltage stability and enhance PQ in the presence of D-STATCOM [16]. However, the GWO was suggested to optimize the gain parameters of PIC based UPQC to reduce THD for both linear and non-linear loads [17]. A PIC was adopted to stabilize the DLCV for SHAPF to successfully address PQ problems by adopting hysteresis current control for pulse generation. Additionally, performance was studied on both linear and non-linear loads [18]. The BBO was selected to obtain optimal gain values of PIC and for fast action in fault identification with higher accuracy with a motive of stabilizing DLCV fluctuations [19].

The hybrid fuzzy ANN-based control technique was adopted for UPQC to minimize the current THD and voltage fluctuations and improve network usage [20]. The Improved bat and Moth Flame metaheuristic optimization methods were hybridized to solve the PQ issues by optimal selecting the gain values of PIC [21]. The FLC was developed for SEAF of the distribution network to minimize the current and voltage-related PQ problems [22].

The predator-prey firefly algorithm was selected for the optimal selection of gain parameters of PIC adapted to the SHAPF to reduce the THD and to enhance the PF [23]. A Soccer match optimization for the optimal selection of weights for the ANN controller was suggested for PV/battery-associated UPQC to solve PQ issues [24]. The ACO was chosen for selecting the K_p, K_i values of PIC for the SHAPF to reduce THD under several loading conditions [25]. An self adaptive hysteresis control band in association FLC was designed to the PV-associated 9-level VSC based UPQC to obtain distortions free voltage signal [26]. Besides, the Soccer-league optimization was proposed for the optimal selection of PIC gain parameters for UPQC to successfully handle both voltage fluctuations and current distortions [27].

The hybrid control technique with both characteristics of FLC and ANN was recommended for UPQC to minimize the grid voltage and current waveforms imperfections with DLCV balancing for dynamic loads [28]. The ANN based method was suggested for five-level UPQC to address the PQ issues effectively [29]. The firefly optimization was used to train ANNC was developed for the shunt VSC for the PV/battery UPQC to reduce the MSE and minimise THD [30]. The self tuning filter based method was developed for UPQC integrated with renewable sources to address PQ issues [31]. The LMBP-trained ANN controller was adopted for UPQC to mitigate current and voltage-related PQ problems efficiently [32]. A two-tier cascaded system was developed for fault finding as well as fault categorization in the local electrical distribution system [33]. An AC-O was suggested to analyze congestion management to obtain the optimal place for allocation of TCSC, for IEEE 14-bus test system while satisfying the constraints [34]. A economic, technical, and environmental study was conducted while taking investment, installation and working costs of PV system in addition to the penalty rates of emission of CO2 with a aim of supplying the electricity to Iran [35].

It was investigated [36] the advantages and difficulties of integrating renewable energy sources into the system and their control strategies. A few recommendations were also made to transform the conventional grid into a smart grid, and the implications of smart grid technologies on the national grid were underlined [37]. For changes in solar irradiation, the comparison of P & O and PSO algorithms to provide MPP for the PV system was investigated [38]. Integration of renewable sources to micro grid for MPPT was studies with power management [39]. High voltage isolated ACDC converters were developed based on the modular technology [40]. Fuzzy logic controller was suggested for PV-MPPT to improve the overall performance by maximum power point tracking [41].

From the Table-1 literature, it is very clear that Most of the recent literature papers mainly focused on various controllers with the existing conventional control schemes for UPQC containing the complex parks and Clarke's transformations. This manuscript develops an ANN based reference signal generation for PV/battery connected DClink UPQC in addition to ANFIS controller for DC link balancing.

The novelty of this manuscript is highlighted in the steps below:

- Developing the Diode clamped five level VSC for UPQC for effectively reducing imperfections in waveforms effectively.

- Introducing the levenberg marquardt trained ANNC for generating effective reference signals in order to eliminate the necessity of complex abc-dq0-αβ0 conversions i.e SRF and p-q theories.
- Proposing the hybrid ANFIS controller to maintain constant DLCV.
- Incorporating the solar PV and battery systems to the DC link of 5L-UPQC to reduce the stress and burden on VSC, supports to meet the load demand, and maintain constant DLCV during load variations.
- The objective of the proposed system is to diminish the source current THD, and eliminating the grid voltage side troubles like (disturbance, swell, sag etc.)
- Additionally, the suggested ANFIS scheme for 5L-UPQC with PV and BES (5L-UPVBES) is examined on two test cases for different loading conditions to show it's superior performance.
- The concert was tested by comparing it with PIC, and SMC techniques.

This paper is structured as follows, section2 gives the modeling of 5L-UPVBES, Section 3 explains the proposed control scheme, Section 4 demonstrates the results and discussion, and Section 5 concludes the manuscript.

2. Modelling of Developed 5L-UPVBES

The proposed 5L-UPVBES configuration is displayed in Figure 1 where PV and battery is connected to UPQC's DC link. UPQC is the combination of series and shunt VSCs. The SAPF intends to eliminate grid-side voltage-related problems by supplying the suitable compensation voltage through the injecting transformer via the inductor. Similarly, the SHAPF is connected through the interfacing inductance to the grid. The SHAPF aims to reduce the current waveform harmonics and to maintain DLCV constant with minimum settling time by injecting suitable compensating current.

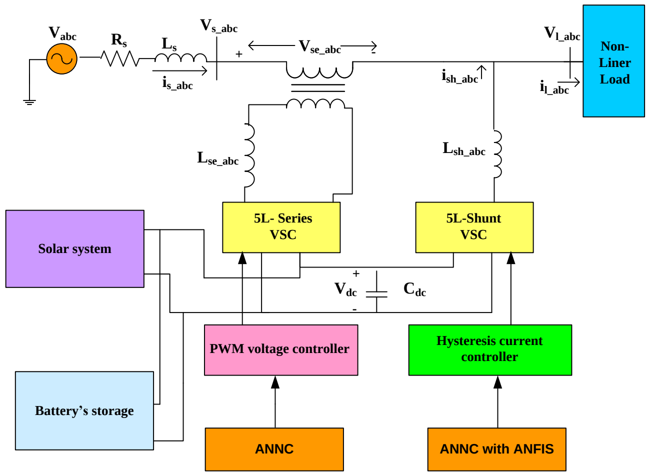

Fig. 1. Proposed 5L-UPVBES configuration

Table 1: A literature survey (current start of art)

Ref/ year	Control		PQ Issues				Loads	
[No]/Year	Reference signal generation	Controller	THD	DLCV balancing	Supply Voltage sag, swell	Supply Voltage disturbance	Non-linear sensitive load	Unbalanced load
[3] / 2020	p-q theory	FOPID	✓				✓	✓
[4]/ 2022	SRF	PIC	✓					
[7]/ 2023	ANN	ANN	✓	✓	✓	✓	✓	✓
[8]/ 2022	SRF	FUZZY-PI	✓	✓			✓	
[11]/ 2021	ANN	ANN	✓		✓		✓	✓
[19]/ 2021	SRF	PI-BBO	✓		✓		✓	✓
[21]/2021	SRF	ANFIS	✓				✓	✓
[22]/2018	p-q	FUZZY	✓		✓		✓	
[23]/ 2019	SRF	PPFFA	✓				✓	✓
[25]/2019	SRF	PI-ACO	✓				✓	✓
[29]/ 2017	ANN	ANN	✓	✓	✓		✓	✓
[30]/2023	SRF	FF-ANN	✓	✓	✓	✓	✓	✓
Proposed 5L-UPVBES	**ANNC**	**ANFIS**	✓	✓	✓	✓	✓	✓

2.1 Selection of C_{dc} and V_{dc}

From [29], under faulty conditions, assume the shunt and series VSC's power handling capacities are 0.5XkVA and 2XkVA, respectively. The kVA rating of VSC and V_{dc} is inversely proportional. By the change of 25% of V_{dc}, the equivalent change in the energy across C_{dc} is calculated by Eq. (1)

$$\Delta E_{dc} = 1/2C_{dc}[(1.125V_{dc})^2 - (0.875V_{dc})^2] \quad (1)$$

Assume that for the suppose the load changes from 2XkVA to 0.5XkVA in '*n*' cycles in '*T*' sec, then the corresponding change in the system's energy is given by

$$\Delta E_s = (2X - X/2)n.T \quad (2)$$

By, equating Eq. (1) and (2), the C_{dc} is given by Eq. (3)

$$C_{dc} = \frac{2(2X - X/2)n.T}{(1.125V_{dc})^2 - (0.875V_{dc})^2} \quad (3)$$

Let, V_{dc} is m times to V_m. Where, '*m*' modulation index varies between 1.2 and 2. However, %THD depends on L_{sh} and V_{dc} so the value of m is selected as 1.6 [29] for minimum THD. Therefore, V_{dc} is given by Eq. (4)

$$V_{dc} = 1.6 * V_m \quad (4)$$

The V_{dc} for *n* level converter is evaluated by using [29] Eq. (5)

$$V^{ref}{}_{dc} = V_{dc}/(n-1) \quad (5)$$

2.2 Selection of Coupling Inductors for Shunt and Series VSC

The coupling inductors adopted to connect the series and shunt VSC's to the source and the load are limited by di/dt and magnitude of currents. The Δi_{lmax} occurs at *m*=0.5, given in Eq. (6) is controlled by PWM [29].

$$\Delta i_{l\max} = V_{dc}/6 f_{sw} L_{se} \quad (6)$$

Assuming the ripple current is about 10% of the maximum peak-to-peak current given by Eq. (7)

$$\Delta i_{l\max} = 0.1 * i_{\max} \quad (7)$$

Therefore, the maximum current handling by a series capacitor in terms of power and phase voltage is given by Eq. (8). By using Eq. (6) and (8) L_{se} can be calculated.

$$i_{\max} = \frac{\sqrt{2} * P_r}{3 * V_{ph}} \quad (8)$$

By heuristically testing [29] it has been identified that for *m*=1.6, $V^{ref}{}_{dc}$= 700, and L_{sh}= 15 mH the % THD is lower. The value of L_{sh} is given by Eq. (9)

$$i_{\max} = \frac{V_{dc}}{4.h.f_{sw\max}} \quad (9)$$

Where, h is the hysteresis band 5-10%.

2.3 Modelling of External Support of 5L-UPQC

The solar/battery-fed DC link is proposed for the diode clamped 5L-UPQC. It consists of a hybrid solar and battery energy system to regulate the DLCV during the variation in loads. External support can reduce the converter ratings and stress by lowering the utility's demands. The equation for DC link power demand (P_{dc}) of the suggested technique is given in equation (10).

$$P_{PV} + P_{BSS} - P_{dc} = 0 \quad (10)$$

2.3.1 Solar Power Generation System (SPG)

In this work, PV model is taken from the Simulink library. The PV models are connected in series to form a string, and some of such strings are connected in parallel to generate the required amount of voltage and current. Every PV cell is modelled in the module using a single diode equivalent circuit [31] as shown in Fig 2. It consists of photo current source (i_{ph}) with forward diode carrying current (i_d), a series and parallel cell resistances ($R_{s,PV}$ and $R_{sh,PV}$) carrying current of (i_{PV}, $i_{sh,PV}$). The PV cell identifies sun irradiation and converts it into current. Practically, PV cells are aligned in groups in larger number called PV modules. However, these modules are connected in series or parallel depending on the requirement to create PV arrays which are used to generate electricity in PV generation systems. PV module photo current source (i_{ph}) is obtained by Eq. (11) and PV module reverse saturation current i_{rs} is given by Eq. (12)

$$i_{ph} = [i_{SC} + K_i(T - 298)] * G/1000 \quad (11)$$

$$i_{rs} = i_{SC}/[\exp(qV_{oc}/N_s \eta k T) - 1] \quad (12)$$

Here, i_{SC} is the short circuit current, K_i is i[th] cell short circuited current, *q* is the electron charge, η is the diode ideal factor, *k* Boltzmann's constant and *T* denotes the cell temperature, G is the solar irradiation, V_{oc} is the open circuit voltage and N_s, N_p are the series and parallel connected PV cells to form module.

The module saturation current depends on cell temperature which is given by Eq. (13) and output current of module is given by Eq. (14).

$$i_{mo} = i_{rs}[T/T_n]^3 \exp[q * E_g/\eta k(1/T - 1/T_n)] \quad (13)$$

$$i_{PV} = N_p * i_{ph} - N_p * i_{mo} * [\exp(V_{pv}/N_s + i_{PV} * (R_{s,PV})/\eta V_t) - 1] - i_{sh,PV} \quad (14)$$

Where,

$$V_t = k * T/q$$
$$i_{sh,PV} = V_{PV} * ((N_p/N_s) + i_{PV} * R_{s,PV})/R_{sh,PV} \quad (15)$$

Here, T_n is the nominal temperature, E_g is the band gap of semi conductor. The output power obtained by the solar system (P_{PV}) is calculated by equation (16). The solar cell characteristics for constant temperature and variable irradiation is exhibited in Fig. 3

$$P_{PV} = V_{PV} \times i_{PV} \quad (16)$$

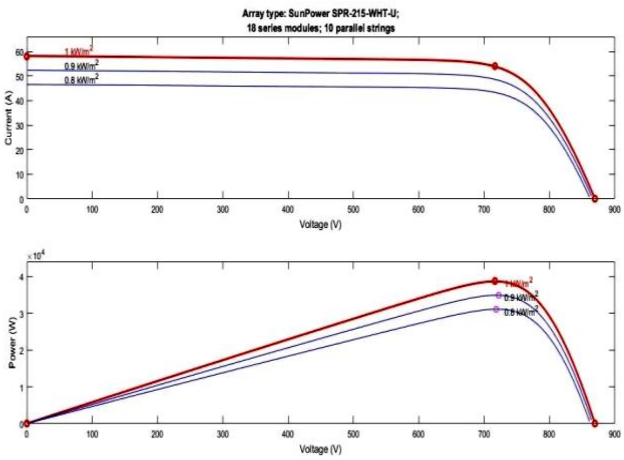

Fig.3. PV cell characteristics at various irradiation and constant temperature 25^{0}c

2.3.2 Battery Storage System (BSS)

The BSS provides support in stabilizing the DLCV. Battery consists of cells arranged in series or parallel to achieve the desired voltage and current. This work selects Li-ion batteries from the Simuink library due to its advantages like slow discharge and low maintenance cost. The charging/discharging model of the Li-ion battery is in Eq. (17)

$$V_b = V_{b\_charge,b\_discharge}(i_t, i^*, i_b) - i_b R \quad (17)$$

Where, $V_{b\_charge,b\_discharge}$ is the battery charge and discharge voltage, R is the internal battery resistance, i_b battery current. The charge and discharge of Li-ion type battery is expressed in terms of constant voltage E_0 (Volts) , R internal resistance and battery capacity Q, K is the polarization constant given by Eq. (18).

$$E_{b\_charge} = E_0 - K\left(\frac{Q}{0.1Q + i_t}\right)i^* - K\left(\frac{Q}{Q - \int i_t dt}\right)i_t + Ae^{-b^* i_t} - i_b * R \quad (18)$$
$$E_{b\_discharge} = E_0 - K\left(\frac{Q}{Q + i_t}\right)i^* - K\left(\frac{Q}{Q - \int i_t dt}\right)i_t + Ae^{-b^* i_t} - i_b * R$$

The state of charge of battery (*SOCOB*) is expressed in Eq (19).

$$SOCOB = 50\left(1 + \int i_{BSS}\ dtQ\right) \quad (19)$$

The SPG will decide whether the battery to charge or discharge while satisfying the constraints given by Eq. (20). The discharge of the battery is shown in Fig. 4. The rating selected for solar and battery systems are listed in Table 2.

$$SOCOB_{\min} \le SOCOB \le SOCOB_{\max} \quad (20)$$

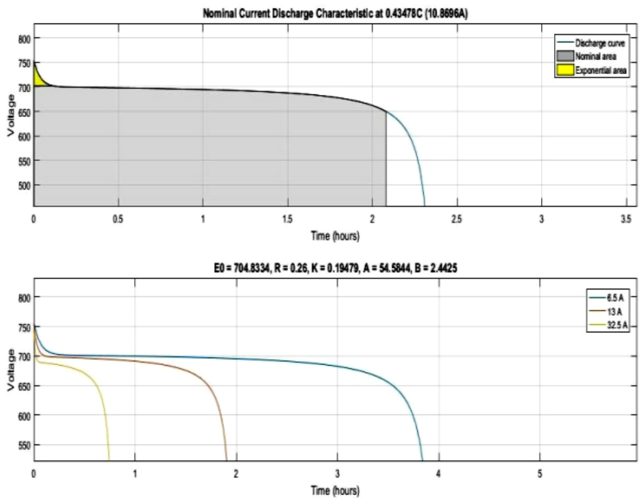

Fig. 4. Li-ion battery characteristics for discharge

Table 2: Solar and BSS Ratings

Equipment	**Factor**	**Value chosen**
PV single panel (Sun power SPR-215-WHT-U)	Rated Power	214.92W
	Open circuit voltage	48.3V
	Short circuit current	5.8A
	Under max power the voltage & current	39.8V /5.4A
	Number of PV cells assembled in parallel, series	11, 18
Li-ion battery	Rated Capacity of battery	25Ah
	Normal Voltage	650V
	Fully charge voltage	756.59V
	Cut off voltage	487 V

3. Proposed Control Scheme

In general, V_{dc} changes during the dynamic load variation at the distribution side. However, to make the system normal, V_{dc} it is necessary to retain back to its original value for a short duration. Here, the PWM technique produces gate pulses for the series VSC and PWM hysteresis current control for shunt VSC with the suggested ANNC.

3.1 Shunt VSC

The main aim of SHAPF is to suppress the imperfections in current waveforms and to regulate DLCV during faults and dynamic loading conditions by injecting compensating current. The structure of ANN contains an OL, IL, and a HL. Where, IL collects data given as input and transfers it to the HL. Later, it is multiplied with those of respective weight's on the associated links, coupled between the IL and HL. Here, calculations are carried out subjected to selected bias on HL; obtained results are accumulated in OL.

Here, LMBP-based ANN is selected. The link's weights are modified during training by evaluating the error to obtain the desired output. The LMBP training technique is adopted for ANN training where the performance function is MSE. LMBP algorithm uses resulting derivatives for weigh updating, which possesses the characteristics of efficient learning and faster convergence [32].

3.1.1 ANFIS

The ANFIS is suggested to maintain constant DLCV. The suggested ANFIS is an intelligent hybrid controller with a combination of ANN and Fuzzy logic features. However, for maintaining DLCV constant, the chosen reference DLCV is compared to the obtained DLCV; its output E, CE is considered as input. The inputs fed to the ANNC are initially trained according to the Gaussian MSF to produce the best as shown in Figure 5. ANFIS mainly consists of five layers, the 1^{st} layer (Fuzzification) the outputs of this layer are fuzzy MSF given by Eq. 21 shown in Fig. 7

$$\mu_{Ai}(x), i = 1,2.$$
$$\mu_{Bj}(y),\ j = 1,2. \quad (21)$$

Where, μ_{Ai} μ_{Bj} are the MSF outputs obtained from the 1^{st} layer.

The mathematical representation of Gaussian MSF is given by Eq.22

$$\mu(x) = e^{-(\frac{x-a}{b})^2} \quad (22)$$

The Negative-Big (NEB), Negative medium (NEM), Zero (ZOE), Positive small (PES), Positive Big (PEB), Positive medium (PEM) and Negative-Small (NES) are considered as input. The inputs of MF are shown in Fig 6. Table 3 exhibits the fuzzy-rule-base.

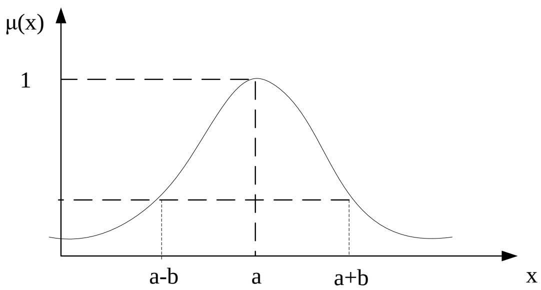

Fig.5. Gaussian MSF

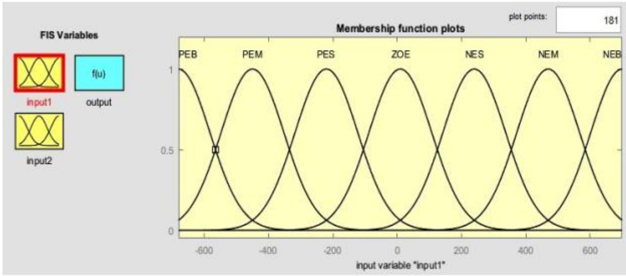

(a) MF for E

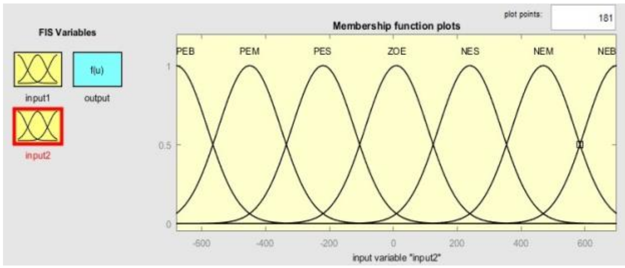

(b) MF for CE

Fig.6. Fuzzy MFS for E, CE

Table 3: Fuzzy Rule-base

E	CE						
	PEB	PEM	PES	ZOE	NES	NEM	NEB
NEB	ZOE	NES	NEM	NEB	NEB	NEB	NEB
NEM	PES	ZOE	NES	NEM	NEB	NEB	NEB
NES	PEM	PES	ZOE	NES	NEM	NEB	NEB
ZOE	PEB	PEM	PES	ZOE	NES	NM	NEB
PES	PEB	PEB	PEM	PES	ZOE	NES	NEM
PEM	PEB	PEB	PEB	PEM	PES	ZOE	NES
PEB	PEB	PEB	PEB	PEB	PEM	PES	ZOE

However, in the 2^{nd} layer (weighting of fuzzy rules) the AND operator is applied and calculates the firing strength w_i by adopting MSF computed in 1^{st} layer, whose output is calculated by Eq. (23).

$$w_k = \mu_{Ai}(x) * \mu_{Bj}(y) i,\ j = 1,2. \quad (23)$$

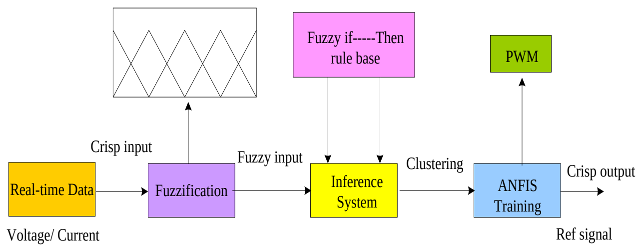

Fig.7. Overview of ANFIS

The normalization of values occurs in the 3^{rd} layer received from the previous layer. Each node reaches normalization by evaluating the ratio of the k^{th} rule's firing strength (truth values) to the summation of all rule's firing strength is given Eq. (24).

$$\overline{w_k} = \frac{w_k}{w_1 + w_2} k = 1,2. \quad (24)$$

The self-adaptive ability of the ANNC is carried out by applying the inference parameters (p_k, q_k, r_k) in the 4th layer (defuzzification) output is given by Eq. (25).

$$\overline{w_i} f_i = \overline{w_i}(p_k u + q_k v + r_k) \qquad (25)$$

Lastly, at the 5th layer, inputs are get added up to produce the desired total ANFIS output by Eq. (26).

$$f = \sum_i \overline{w_i} f_i \quad (26)$$

Fig 8 shows the block diagram of the proposed ANFIS.

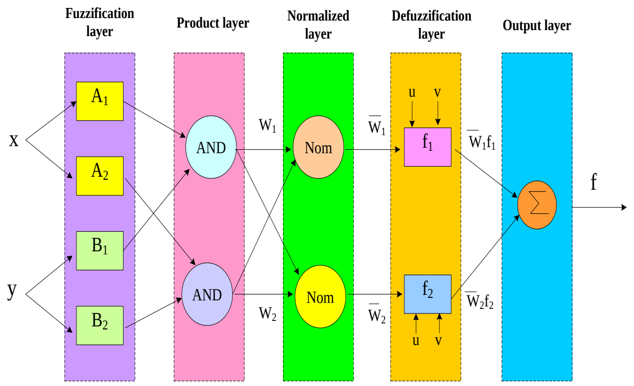

Fig. 8. Structure of ANFIS

The ANFIS is trained to maintain constant DLCV and to generate reference current signals. However, for keeping the DLCV constant, reference DLCV (V^{ref}_{dc}) is compared with the actual DLCV (V_{dc}) ; its error is chosen as input data, Δi_{dc}. Next, the load currents, like (i_{l_abc}) and DC loss component (Δi_{dc}), are considered as input while the reference currents ($i^{ref}_{sh\_abc}$) are considered as target data as shown in Figure 9, and the structure with neurons selected are shown in Fig 10.

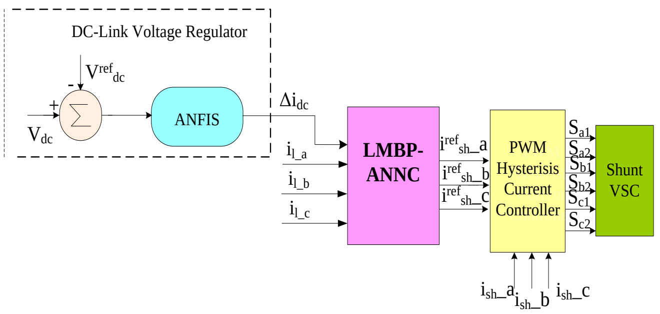

Fig. 9. Shunt VSC Controller

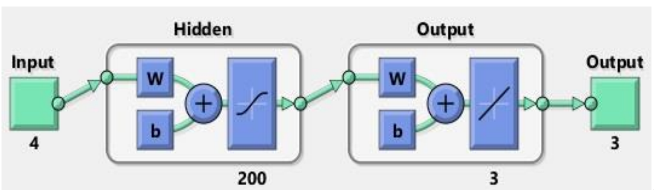

Fig. 10. Structure of ANNC for reference current generation.

3.2 Series VSC

The prominent role of SAPF is to suppress the grid side voltage distortions by injecting the suitable compensating voltage to maintain load voltage constant. Figure 11 exhibits the suggested series VSC reference signal generation scheme and Figure 12 shows the structure of ANN with a HIL of 200 neurons. To generate the reference voltage signals ($V^{ref}_{se\_abc}$) the supply voltages (V_{s_abc}) are considered as input data, while reference voltage is deemed into target data to ANN. The gating pulses for series VSC are generated with PWM.

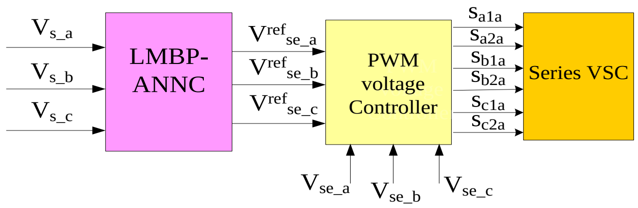

Fig. 11. Series-VSC controller

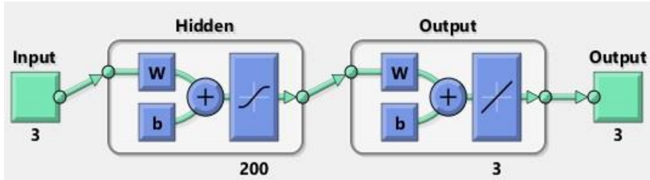

Fig. 11. Structure of ANNC for reference voltage generation.

4 Simulation and Results

The proposed 5L-UPVBES with ANNC was designed in Matlab 2016a and implemented in Intel core-i5, 2.67 GHz, 8GB DDR. The Simulink model of the proposed method is given in Figure 13. In Figure (a) illustrates the 5Level diode clamped VSC model for UPQC, and Figure (b) provides the proposed ANNC control scheme adopted for shunt and series converters. The selected system and the UPQC device parameters chosen are displayed in Table 4. However, two test cases with various permutations of voltage issues like sag, disturbance, swell, balanced and unbalanced loads with constant irradiation (G) and temperature of 25^0c were selected to revel the working of developed ANNC on 5L-UPVBES is given in Table 5. The voltage sag, voltage swell, and voltage disturbance issues are considered for both case-1 and 2. However, in this work the reduction of current THD is regarded as objective which is obtained by developed ANN for reference signal generation, and optimal selection of shunt and series controller parameters for diode clamped 5L-UPQC. The comparative analysis is carried out with PIC and SMC methods at DLCV balancing. The THD is evaluated by Eq. (27).

$$THD = \frac{\sqrt{(I^2{}_2 + I^2{}_3 + ...I^2{}_n)}}{I_1} \qquad (27)$$

Where,

I_n= individual harmonic current distortion values in amps

I_1= individual harmonic current distortion values in amps

I_2= 2nd harmonic current distortion values in amps

The voltage sag/ swell ($V_{sag/swell}$) is evaluated by Eq. (28)

$$V_{sag/swell} = \frac{V_l - V_S}{V_l} = \frac{V_{se}}{V_l} \qquad (28)$$

The injected voltage by series filter is calculated by Eq. (29)

$$V_{se} = V_l - V_S \qquad (29)$$

The injected current by shunt filter is calculated by Eq. (30)

$$i_{sh} = i_i - i_S \quad (30)$$

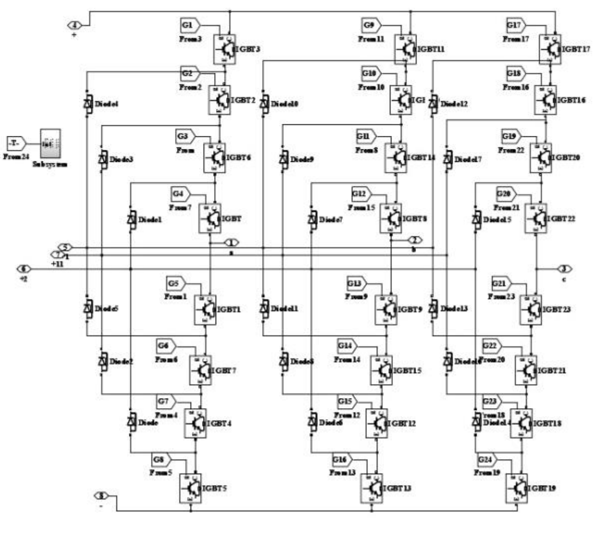

(a) Diode clamped 5-level VSC

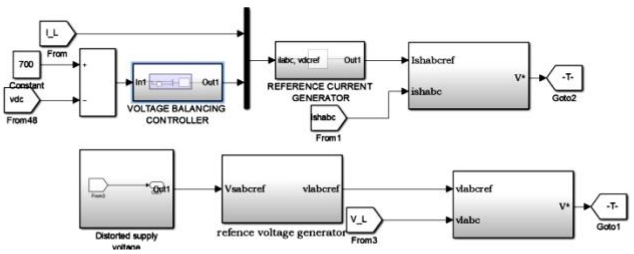

(b) Proposed ANN with ANFIS-based reference signal generation scheme

Fig.13. Simulink model of the proposed system

Table 4: System and 5L-UPQC parameters

Grid Supply	V_S : 415Volts ; f : 50Hertz R_S : 0.1ohm ; L_S : 0.15 mH
DC link capacitor & coupling inductors	C_{dc}: 2200µF; L_{se}= 6 mH, L_{sh}=15 mH
Loads	1. Balanced3 Φ nonlinear load: P_L=3kW, Q_L=0.5 kVAR 2. Un-balanced load: P_{La}=3kW, Q_{La}=9 kVAR; P_{Lb}=4kW, Q_{Lb}=10 kVAR; P_{Lc}=4kW, Q_{Lc}=10 kVAR

Table 5: Test Cases studies considered for different loads

Condition	Case1	Case2
Balanced V_S	✓	✓
Source voltage V_{Sag} ,V_{Swell} , disturbance	✓	✓
Current	✓	✓
Constant Irradiation 1000W/m2 and 25^{0}c temperature	✓	✓
THD (both V and I)	✓	✓
Load1	✓	
Load 2	✓	✓

In case1, 30% of sag/ swell and a disturbance is created in supply voltage for 0.2 to 0.3 sec, 0.4 to 0.5sec, and 0.6 to 0.7 sec, respectively as shown in Fig 14(a). The developed ANN technique effectively notices the voltage dip, voltage raise, and disturbance, supplies the required compensating voltage through the interfacing transformer and maintains the load voltage constant. Besides, to exhibit the behavior of the shunt filter with ANNC, Loads 1 and 2 were considered. The load current waveform is unbalanced and non-sinusoidal, as seen in Fig 14(b). The developed method suppresses the distortions in the source current, reducing the THD of source current to 2.23% and load voltage to 0.37%, much less than other techniques. In addition, it regulates DLCV stable as shown in Fig 14(c) for constant 1000W/ m2 irradiation and 25^{0}c of constant temperature.

In case 2, similar to case 1, the disturbance is introduced to the 30% of balanced sag and swell. However, the proposed system identifies it successfully and eliminates it by injecting the required compensating voltage, as illustrated in Figure 15(a). The load current waveform was sinusoidal but unbalanced as shown in Figure 15(b), due to unbalanced load 2. However, the proposed method reduces the THD of the source current to 3.64% and load voltage to 0.20, which is lesser than other techniques. However, the suggested method maintains constant DLCV, as Figure 15(c) shows. Table 6 compares the THD of the proposed method with those of other standard methods like PIC and SMC, and other controllers in the literature survey. It exhibits that the proposed method has much lower THD when compared to other techniques. However, Figure 16 represents the FFT analysis of the current proposed system.

In addition, it is observed that along with load variation as studied in case studies the solar irradiation remains constant for 0 to 0.3sec and varies till 0.7 under constant temperature condition as shown in Figure 17. The proposed system works effectively and maintains constant voltage during irradiation variation conditions. From the results analysis it is clearly exhibited that the proposed 5L-UPQC based ANN controller based reference signal generation technique effectively works in reducing imperfections in the waveforms and improves THD in addition to the elimination of complex SRF and p-q transformations. Moreover, it also works well during load and solar variations effectively.

Table 6: THD comparison

	Method [Ref]	THD					
		Source Current			Load Voltage		
		Phase-a	Phase-b	Phase-c	Phase-a	Phase-b	Phase-c
Case-1	**Proposed method (ANN with ANFIS)**	**2.23**	**2.46**	**2.41**	**0.21**	**0.77**	**0.74**
	ANNC	2.65	2.81	2.80	0.37	0.67	0.75
	PIC	3.06	3.05	3.06	4.05	3.54	2.55
	SMC	2.84	2.84	2.82	4.07	4.39	4.01
	2L-UPQC [29]	5.42	5.43	5.61	4.03	3.86	4.04
	3L-UPQC [29]	4.72	4.45	4.86	3.37	3.27	3.36
	5L- UPQC [29]	3.85	4.09	4.40	3.02	2.97	3.03
	2L-UPQC-SRF [29]	5.47	6.07	5.95	4.45	4.76	4.99
	3L-UPQC-SRF [29]	5.55	6.06	4.94	4.22	4.24	4.43
	5L-UPQC-SRF [29]	4.55	5.45	4.32	3.83	3.98	4.22
	ANN [7]	3.72	--	--	--	--	--
Case-2	**Proposed method (ANN with ANFIS)**	**3.64**	**3.76**	**3.70**	**0.20**	**0.83**	**0.80**
	ANNC	3.83	3.89	3.90	0.36	0.66	0.75
	PIC	4.06	4.12	4.02	4.05	3.54	2.55
	SMC	3.98	3.98	3.99	2.89	4.12	3.47
	ANN [7]	4.55	--	--	--	--	--

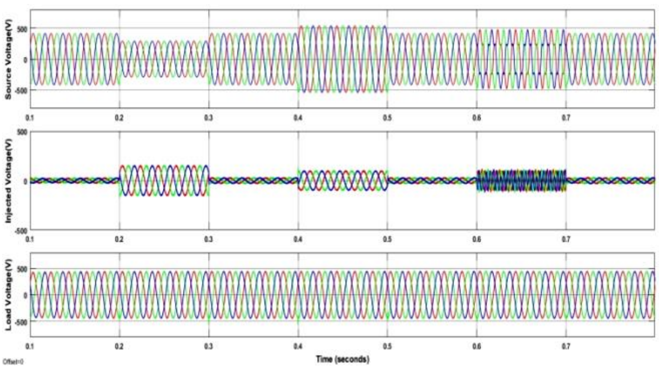

(a) V_S , V_{se} , V_l

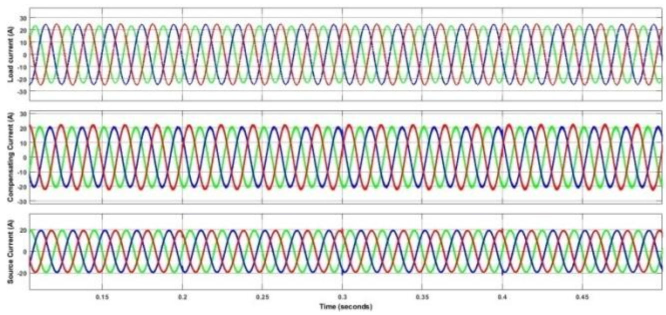

(b) i_l , i_{sh} , i_S

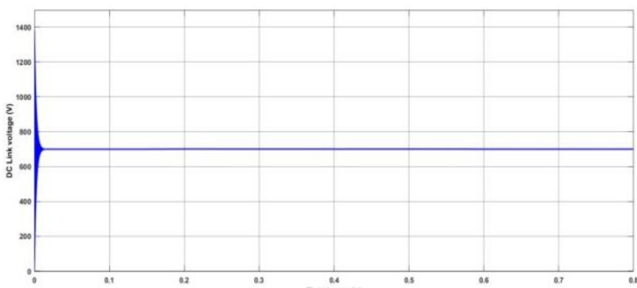

(C) DLCV

Fig.14. Waveforms of developed method for case-1

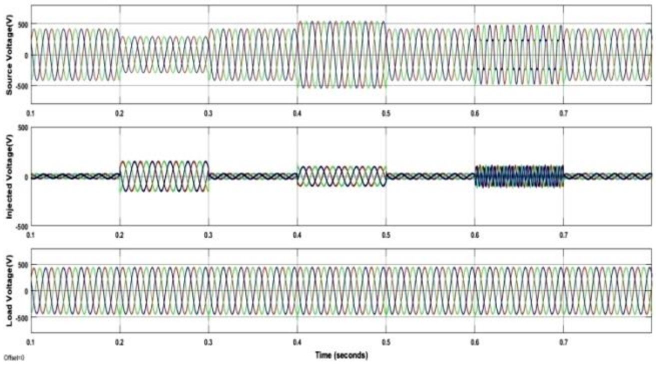

(a) V_S , V_{se} , V_l

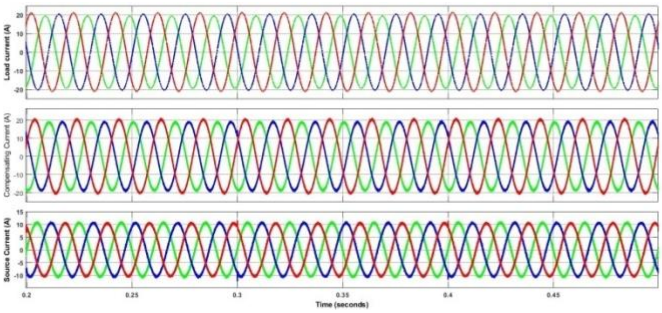

(b) i_l , i_{sh} , i_S

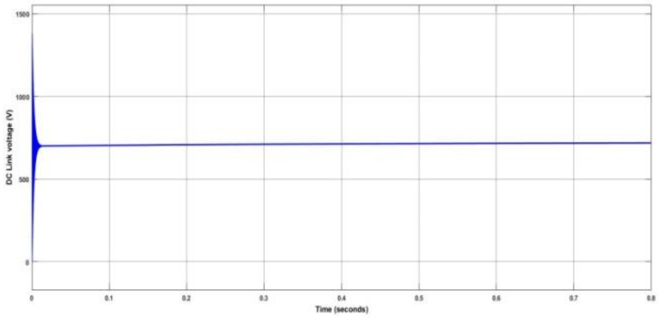

(c) DLCV

Fig.15. Waveforms of developed method for case-2

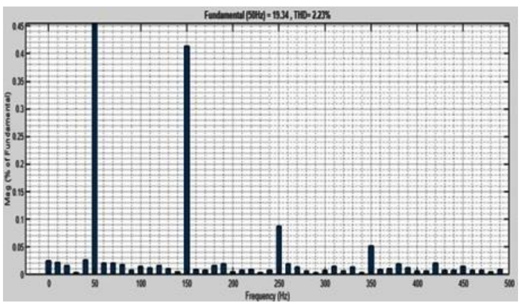

(a) Case-1

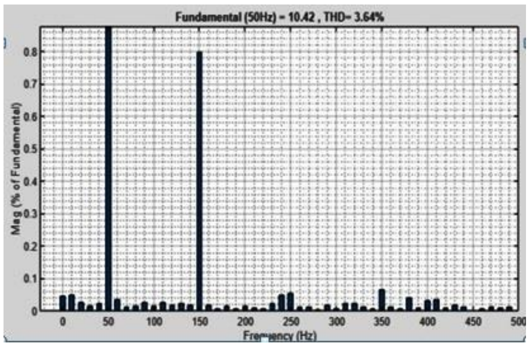

(b) Case-2

Fig.16. THD spectrum for case studies

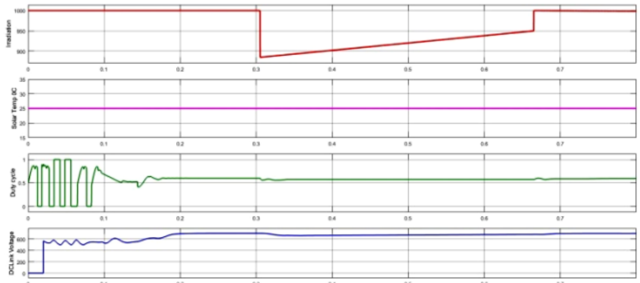

Fig. 17. During load-1 (a) variable G (b) 25^{0}c constant T(c) DLCV

5 Conclusion

This paper proposes an ANNC-based new method for a solar battery connected to UPQC. The LMBP-trained ANN controller is presented to produce the required reference signals for shunt series VSC's to avoid the traditional abc-dq0-αβ conversions. In addition, the ANFIS hybrid controller is adapted for DLCV balancing. However, the developed diode clamped 5L-UPVBES maintains constant DLCV during loads variations, suppresses the source current and load voltage harmonics and improves the current and voltage waveform's shape, and eliminates the fluctuations of supply voltage (disturbance, sag and swell). The comparison is carried out with ANN, PIC and SMC controllers for DLCV balancing and other methods available in the literature. The results of the two test cases show that the developed method provides much lower THD than other methods in literature and within acceptable levels. The developed method can be carried out using metaheauristic optimization control scheme in the future in addition to the microgrid.

References

1. D. Yang , Z. Ma , X. Gao , Z. Ma, E. Cui, "Control Strategy of Intergrated Photovoltaic-UPQC System for DC-Bus Voltage Stability and Voltage Sags Compensation", Energies, Vol. 12, No. 20, pp. 4009, Oct-2019.
2. G Arunsankar, and S. Srinath, "Optimal controller for mitigation of harmonics in hybrid shunt active power filter connected distribution system: An EGOANN technique", Journal of Renewable and Sustainable Energy, Vol. 11, No. 2, pp. 025507, April-2019.
3. A. Mishra , S. R. Das , P. K. Ray , R. K. Mallick, A. Dillip ,K. Mishra, "PSO-GWO Optimized Fractional Order PID Based Hybrid Shunt Active Power Filter for Power Quality

Improvements", IEEE Access, Vol.8, pp. 74497 - 74512, May-2020

4. D. Mahdi and G. Gorel, "Design and Control of Three-Phase Power System with Wind Power Using Unified Power Quality Conditioner", Energies 2022, Vol. 15, No. 19, pp. 7074, Sep-2022.
5. X. Zhao ,X. Chai, X. Guo, A. Waseem, X. Wang and C. Zhang, "Impedance Matching-Based Power Flow Analysis for UPQC in Three-Phase Four-Wire Systems", Energies, Vol.14, No. 9, pp. 2702, May-2021
6. Y. Hoon, M. A. MohdRadzi, M. Hassan, N.F. Mailah, "Control Algorithms of Shunt Active Power Filter for Harmonics Mitigation: A Review", Energies, Vol.10, No.12, PP. 2038, Dec-2017.
7. K. Srilakshmi, K. K. Jyothi, G. Kalyani & Y. S.P Goud. "Design of UPQC with Solar PV and Battery Storage Systems for Power Quality Improvement. Cybernetics and Systems: An International Journal", March-2023.
8. T. Chiao Lin, B. Simachew, "Intelligent Tuned Hybrid Power Filter with Fuzzy-PI Control", Energies, Vol. 15, No. 12, pp. 4371, June-2022.
9. O.E Okwakol , Z. Hui Lin 1, M. Xin, K. Premkumar, Alukaka, "Neural Network Controlled Solar PV Battery Powered Unified Power Quality Conditioner for Grid Connected Operation", Energies, Vol. 15, No. 18, PP. 6825, Sep-2022.
10. M. Moazzami, G. B. Gharehpetian, H. Shahinzadeh and S. H. Hosseinian, "Optimal locating and sizing of DG and D-STATCOM using Modified Shuffled Frog Leaping Algorithm," 2017 2nd Conference on Swarm Intelligence and Evolutionary Computation (CSIEC), Kerman, Iran, 2017, pp. 54-59.
11. K. Chandrasekaran, J. Selvaraj, C. Amaladoss, L. Veerapan, "Hybrid renewable energy based smart grid system for reactive power management and voltage profile enhancement using artificial neural network, Energy Sources, Part A: Recovery, Utilization, and Environmental Effects", Vol. 43, No. 19, pp. 2419–2442, sep-2022.
12. B. Aljafari, K. Rameshkumar, V. Indragandhi, S. Rama chandran, "A Novel Single-Phase Shunt Active Power Filter with a Cost Function Based Model Predictive Current Control Technique", Energies, Vol.15, No. 13, pp. 4531, Jun-2022.
13. K. Sarker, D. Chatterjee & S. K. Goswami, "A modified PV-wind-PEMFCS-based hybrid UPQC system with combined DVR/STATCOM operation by harmonic compensation", International Journal of Modeling and Simulation, Vol.41, No.4, pp. 243-255, March 2020.
14. Y. Hoon, M. A. Mohd Radzi, M. A. A. Mohd Zainuri, M. Zawawi , "Shunt Active Power Filter: A Review on Phase Synchronization Control Techniques", Electronics, Vol. 8, No. 7, pp. 791, July-2019.
15. A. Szromba, "The Unified Power Quality Conditioner Control Method Based on the Equivalent Conductance Signals of the Compensated Load", Energies, Vol. 13, No. 23, pp. 6298, Nov-2020.
16. A. Nafeh , A. Heikal , R. A. El-Sehiemy, W. A.A. Salem, "Intelligent fuzzy-based controllers for voltage stability enhancement of AC-DC micro-grid with D-STATCOM", Alexandria journal of Engineering, Vol.61, No. 3, pp. 2260-2293, March-2022.
17. M. Nicola, C. Nicola, D. Sacerdoțianu and A. Vintilă, "Comparative Performance of UPQC Control System Based on PI-GWO Fractional Order Controllers, and Reinforcement Learning Agent", Electronics, Vol. 12, No. 3, pp. 494, Jan-2023.
18. A. A. Imam, R. Sreerama Kumar, Yusuf A. Al-Turk, "Modeling and Simulation of a PI Controlled Shunt Active Power Filter for Power Quality Enhancement Based on P-Q Theory", Electronics, Vol. 9, No. 4, pp. 637, April-2020.
19. Sayed J.A, R. A, Sabha, K. J. Ranjan, "Biogeography based optimization strategy for UPQC PI tuning on full order adaptive observer based control. IET Generation", Transmission & Distribution, Vol. 15, No.2 pp. 279-293, Jan-2021.
20. U.K. Renduchintala, C. Pang, K.M. Tatikonda, L. Yang, "ANFIS-Fuzzy logic based UPQC in interconnected microgrid distribution systems: modeling, simulation and implementation", The Journal of Eng, Vol. 2021, No. 1, pp. 6–18, Feb-2021.
21. Rajesh, P, Shajin, F.H, Umasankar. L, "A Novel Control Scheme for PV/WT/FC/Battery to Power Quality Enhancement in Micro Grid System: A Hybrid Technique", Energy Sources, Part A: Recovery, Utilization, and Environmental Effects 2021, pp. 1-18.
22. C. Pazhanimuthu, S. Ramesh, "Grid integration of renewable energy sources (RES) for power quality improvement using adaptive fuzzy logic controller based series hybrid active power filter (SHAPF)", Journal of Intelligent & Fuzzy Systems, Vol. 35, No.1, pp. 749–766, July-2018.
23. S. Mahaboob, S. Kumar Ajithan, S. Jayaraman, "Optimal design of shunt active power filter for power quality enhancement using predator-prey based firefly optimization", Swarm and Evolutionary computation, Vol. 44, 522-533, (2019).
24. K. Srilakshmi, C. Narahari Sujatha, P. Balachandran, L. Mihet-Popa, and N. Udaya Kumar, "Optimal Design of an Artificial Intelligence Controller for Solar-Battery Integrated UPQC in Three Phase Distribution Networks", Sustainability, Vol. 14, No. 21, Oct-2022.
25. A. Sakthivel, P. Vijayakumar, A. Senthilkumar , L. Lakshminarasimman, S. Paramasivam, "Experimental investigations on ant colony optimized pi control algorithm for shunt active power filter to improve power quality", Control Engineering Practice. Vol.42, pp. 153-169, Dec-2015.
26. H. Kenjrawy, C. Makdisie, I. Houssamo, N Mohammed, "New Modulation Technique in Smart Grid Interfaced Multilevel UPQC-PV Controlled via Fuzzy Logic Controller", Electronics, Vol.11, No.6, pp. 919, March-2022.
27. K. Srilakshmi, N. Srinivas , B. Praveen , J. Ganesh Prasad Reddy, S. Gaddameedhi, N. Valluri, S. Selvarajan, "Design of Soccer League Optimization Based Hybrid Controller for Solar-Battery Integrated UPQC", IEEE Access, Vol. 10, pp. 107116-107136, Oct-2022.
28. S. Koganti, K.K. Jyothi and S. Salkuti , "Design of Multi-Objective-Based Artificial Intelligence Controller for Wind/Battery-Connected Shunt Active Power Filter, Algorithms, Vol. 15, No. 8, pp. 256, 2022, July-2022.

29. S. Vinnakoti, V. Reddy Kota, "Implementation of artificial neural network based controller for a five-level converter based UPQC", Alexandria Engineering Journal, Elsevier, Vol .57, No. 3, pp.1475-1488, March-2017.
30. A. Ramadevi , K. Srilakshmi , P. Balachandran ,Ilhami Colak , C. Dhanamjayulu , and Baseem Khan, "Optimal Design and Performance Investigation of Artificial Neural Network Controller for Solar- and Battery-Connected Unified Power Quality Conditioner", International Journal of Energy Research, Vol. 2023, PP. 3355124, April-2023.
31. M. A. Mansoor, K. Hasan, M.M. Othman, S. Z. B. M. Noor, and I. Musirin. "Construction and performance investigation of three phase solar PV and battery energy storage system integrated UPQC", IEEE Accesses , Vol.8, pp. 103511 – 103538,
32. Z. Ming, W. Ru, W. Qiang, Cui Jian, "Control Method for Power Quality Compensation Based on Levenberg-Marquardt Optimized BP Neural Networks", 2006 CES/IEEE 5th International Power Electronics and Motion Control Conference.
33. W. Elmasry, M. Wadi and H. Shahinzadeh, "Two-Tier Cascaded Classifiers to Improve Electrical Power Quality," 2022 26th International Electrical Power Distribution Conference (EPDC), Tehran, Iran, Islamic Republic of, 2022, pp. 96-101.
34. Majid Moazzami, Hossein Shahinzadeh, Gevork B. Gharehpetian, Abolfazl Shafiei, "Optimal TCSC placement for congestion management in deregulated power systems using ant lion optimization algorithm**"** International Journal of Robotics and Automation, International Journal of Robotics and Automation (IJRA), Vol.8, No.2, 9, pp. 77-88, June 2014.
35. M. -R. Memar, M. Moazzami, H. Shahinzadeh and D. Fadaei, "Techno-economic and environmental analysis of a grid-connected photovoltaic energy system," 2017 Conference on Electrical Power Distribution Networks Conference (EPDC), Semnan, Iran, pp. 124-130, 2017.
36. F. Ayadi; I. Colak; I. Garip, H. Bulbul, "Impacts of Renewable Energy Resources in Smart Grid", 8th International Conference on Smart Grid, Paris, pp. 183-188, June 2020.
37. I. Colak; R. Bayindir, S. Sagiroglu, "The Effects of the Smart Grid System on the National Grids", 8th International Conference on Smart Grid, Paris, pp. 122-126, June 2020.
38. S. Jaber, A. M. Shakir, "Design and Simulation of a Boost-Microinverter for Optimized Photovoltaic System Performance", International Journal of Smart Grid, Vol. 5, No. 2, pp. 1-9, June 2021.
39. S. S. Dash, "Tutorial 1: Opportunities and challenges of integrating renewable energy sources in smart" 6th International Conference on Renewable Energy Research and Applications , San Diego, CA, USA, 5-8 Nov. 2017.
40. M. Tsai, C. Chu, W. Chen, "Implementation of a Serial AC/DC Converter with Modular Control Technology", 7th International Conference on Renewable Energy Research and Applications, Paris, France, pp. 245-250, Oct. 2018**.**
41. A. Belkaid, I. Colak, K. Kayisli, R. Bayindir, Improving PV System Performance Using High Efficiency Fuzzy Logic Control, 8th International Conference on Smart Grid, Paris, pp.152-156, June 2020.
42.